Patient-Specific Meshless Model for Whole-Body Image Registration

Mao Li[1], Karol Miller[1,2], Grand Joldes[1], Ron Kikinis[3], and Adam Wittek[1]

[1] Intelligent Systems for Medicine Laboratory,
School of Mechanical and Chemical Engineering
The University of Western Australia, Crawley-Perth, Australia
[2] Inst. of Mechanics and Advanced Materials,
Cardiff School of Engineering, Cardiff University, Cardiff, UK
[3] Surgical Planning Laboratory, Brigham and Women's Hospital,
Harvard Medical School, Boston, MA, USA

Abstract. Non-rigid registration algorithms that align source and target images play an important role in image-guided surgery and diagnosis. For problems involving large differences between images, such as registration of whole-body radiographic images, biomechanical models have been proposed in recent years. Biomechanical registration has been dominated by Finite Element Method (FEM). In practice, major drawback of FEM is a long time required to generate patient-specific finite element meshes and divide (segment) the image into non-overlapping constituents with different material properties. We eliminate time-consuming mesh generation through application of Meshless Total Lagrangian Explicit Dynamics (MTLED) algorithm that utilises a computational grid in a form of cloud of points. To eliminate the need for segmentation, we use fuzzy tissue classification algorithm to assign the material properties to meshless grid. Comparison of the organ contours in the registered (i.e. source image warped using deformations predicted by our patient-specific meshless model) and target images indicate that our meshless approach facilitates accurate registration of whole-body images with local misalignments of up to only two voxels.

1 Introduction

Registration of medical radiographic images plays an important role in cancer diagnosis, therapy planning and treatment [1, 2]. Many algorithms that solely rely on image-processing techniques have been successfully validated for registration of images of selected organs [1, 3, 4]. However, such algorithms exhibit important deficiencies in capturing large deformations of soft body organs/tissue and skeletal motion associated with registration of whole-body computed tomography (CT) or magnetic resonance (MR) images. For such problems, application of biomechanical models, that utilise the principles of computational mechanics, has been advocated to compute deformations of soft body organs/tissues to register (align) two images [5-7].

Biomechanics-based image registration has been historically dominated by Finite Element Method (FEM). In practice, the 8-noded hexahedral element is a preferable

F. Bello and S. Cotin (Eds.): ISBMS 2014, LNCS 8789, pp. 50–57, 2014.

choice when building the models as it does not exhibit volumetric locking for incompressible/nearly incompressible materials such as soft tissues [8]. However, for abdominal organs and other anatomical structures with complex geometry, spatial discretisation (meshing) using hexahedral elements requires time-consuming manual corrections even if state-of-the-art software specifically designed for generation of meshes of anatomical geometries is applied [9, 10].

To eliminate tedious hexahedral mesh generation, meshless methods of computational mechanics, that use easy-to-generate computational grids in a form of cloud of points, have been proposed in the literature for patient-specific biomechanical models [11, 12]. In this study, we use Meshless Total Lagrangian Explicit Dynamics (MTLED) algorithm [11-13] previously successfully applied in computing the brain deformations for neuro-image registration [11, 14].

Conventionally, the material properties of body organs/tissues are assigned by dividing (segmenting) CT/MR images into non-overlapping constituents with different material properties. Although attempts have been made to automate segmentation algorithms [15], in practice, time-consuming manual correction that relies on analyst skills and somewhat subjective interpretation of the images is often needed. Following the studies [9, 14] on application of patient-specific biomechanical modelling for CT and MR image registration, we eliminate the need for segmentation by assigning the material properties using fuzzy tissue classification. The fuzzy tissue classification relies on the Fuzzy C-Means algorithm to calculate the material properties using fuzzy membership functions for the specified image intensity clusters (corresponding to types of tissue depicted in the image) for each voxel in the image [14, 16]. Such classification is an automated process, and the number of tissue classes (image intensity clusters) is the only parameter that needs to be defined by an analyst.

In this study, we demonstrate feasibility and accuracy of the proposed approach by applying it to register two whole-body CT image-sets (referred to as source and target set) acquires at different time for the same patient. We conduct verification by comparing the deformations, that align the source image-set to the target one, computed using patient-specific models implemented by means of the MTLED algorithm combined with fuzzy tissue classification and traditionally used finite element method that relies on meshing for spatial discretisation. Accuracy of the proposed meshless approach is evaluated by comparing the organ contours in the registered (i.e. source image warped using deformations predicted by our patient-specific meshless model) and target images.

2 Methods

2.1 Analysed Whole-Body CT Image Dataset

The analysed CT image dataset was acquired from the publicly available Slicer Registration Library database, Case #20: Intra-subject whole-body/torso PET-CT (http://www.na-mic.org/Wiki/index.php/Projects:RegistrationLibrary:RegLib_C20b). The dataset consists of two image sets with original resolution of 1mm×1mm×5mm acquired at different time-points for the same patient. The sagittal sections of the two image sets are shown in Fig. 1.

2.2 Meshless Total Lagrangian Explicit Dynamics (MTLED) Algorithm

As the detailed description of the Meshless Total Lagrangian Explicit Dynamics (MTLED) algorithm has been provided in [11-13], only brief summary is given here. Computational efficiency of the MTLED algorithm has been achieved through application of Total Lagrangian (TL) formulation of computational mechanics [17] for updating the calculated variables and Explicit Integration in the time domain combined with mass proportional damping. In the Total Lagrangian formulation, all the calculated variables (such as displacements and strains) are referred to the original configuration of the analysed continuum. The decisive advantage of this formulation is that all derivatives with respect to spatial coordinates can be pre-computed [17, 18], which reduces the number of floating point operations per time step in comparison to Updated Lagrangian (UL) formulation used in vast majority of commercial dynamic finite element and meshless solvers.

The MTLED algorithm relies on modified Galerkin method. The field variable is approximated and interpolated using moving least-squares (MLS) shape functions over the domain geometry discretised using nodes (points) [12]. Following [12], we use regular hexahedral background grid with one integration point per cell for spatial integration. The grid was generated automatically as we do not require the integration cells to conform to the geometry of the anatomical structures depicted in the images. The accuracy of this approach has been previously confirmed by Horton et al. [12, 14].

To illustrate how the domain volume geometry is discretised, Fig. 2 shows the whole-body model discretised using a “cloud” of nodes.

2.3 Loading

Following our previous study [9], we load the meshless model by applying prescribed displacements (essential boundary conditions) on the vertebrae. We select vertebrae as the areas to determine the displacements and prescribe the essential boundary conditions since they can be reliably distinguished from the surrounding tissue in CT images. The displacements between vertebrae in source and target images are calculated using the built-in rigid registration algorithm in the 3D SLICER (http://www.slicer.org/)— an open-source software for visualisation, registration, and segmentation of medical images developed by Artificial Intelligence Laboratory of Massachusetts Institute of Technology and Surgical Planning Laboratory at Brigham and Women’s Hospital and Harvard Medical School [19].

2.4 Constitutive Properties and Constitutive Model

Following the approach verified in [9], we use fuzzy tissue classification that utilises the Fuzzy C-Means (FCM) clustering algorithm to assign constitutive properties directly from the images based on the intensity of different tissues of anatomical structures depicted in the images [14, 16].

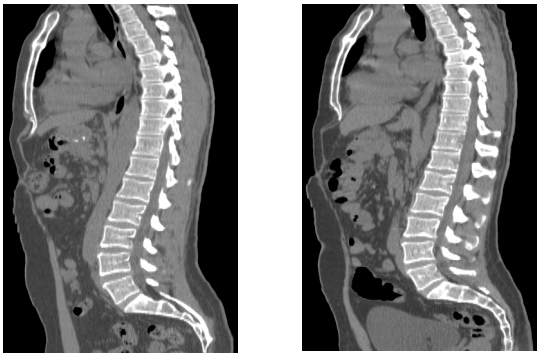

Source Target

Fig. 1. Sagittal sections of whole-body CT image dataset analysed in this study

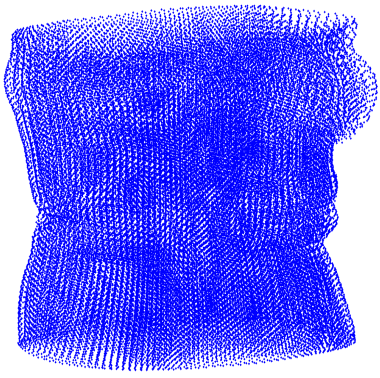

Fig. 2. Whole-body meshless model used in this study. "Cloud" of nodes is used for spatial discretisation.

In the FCM clustering algorithm, each pixel (voxel) in the image is assigned to a number of different tissue types (classes) with different probability. This is done by clustering similar intensity data (pixels) through computation of the membership functions that link the intensity at each pixel with all the specified (i.e. defined by the analyst) cluster centres [14, 16].

There is a vast body of experimental evidence confirming that soft tissues behave like incompressible/nearly incompressible hyperelastic/hyperviscoelastic materials [20, 21]. Therefore, following [20], we used the Neo-Hookean hyperelastic model — the simplest constitutive model that satisfies this requirement. Following [14], the shear modulus G at each integration point of the meshless model was calculated from the FCM-determined membership function u using linear interpolation:

$$G_j = \sum_{k=1}^{C} u_{jk} \times G_k \quad (1)$$

where G_j is the shear modulus at integration point j, G_k is the shear modulus for a given tissue class k, and C is the number of tissue classes (centres of the intensity clusters in the images). Following [9], we use eight clusters (tissue types) with the shear modulus for each class given in Table 1. As the membership function u is computed from pixel intensity, Equation (1) links the information about image intensity with the mechanical properties of anatomical structures depicted in the image.

Table 1. Shear modulus ($\times 10^3$Pa) of different tissue classes for assigning the constitutive properties at integration points using Eq. (1). Note that voxels with different intensity can depict the same tissue (as for lungs and bones in the image datasets analysed here).

Intensity Cluster Centre	-826	-537	-326	-90	-32	43	274	661
Tissue Classes	Lung	Lung	Lung	Fat	Ligament	Muscle	Bone	Bone
Shear Modulus (kPa)	0.53	0.53	0.53	1.07	3.57	4.05	rigid	rigid

3 Results

3.1 Verification of Meshless Models

We verified the computation results (nodal displacements) predicted by means of the proposed patient-specific meshless model implemented using the MTLED algorithm by comparing them with the results predicted using finite element model created and validated in the study by Li et al. [9]. As shown in Fig. 3, for almost all nodes (over 99.5%), the differences between the displacements predicted using the two models are less than 1 mm and the maximum difference is 2.8mm. As these differences are appreciably less than the resolution (1mm×1mm×5mm) of whole-body CT image dataset analysed here, they can be safely treated as negligible.

3.2 Evaluation of Registration Accuracy

Following Li et al. [9] and Mostayed et al. [22], we evaluated the registration accuracy by comparing the edges/contours of the organs in registered (i.e. source image warped using the deformations predicted by our patient-specific meshless model) and target images. As the lung is a large organ that can be reliably distinguished, we qualitatively evaluate the registration accuracy by comparing the contours of the lung extracted from the registered and target images. It can be seen (Fig. 4) that the lung contour extracted from the registered image are very close to those extracted from the target image. The distance between the two contours (registration error) is less than two times of image voxel size of the source image. As the registration accuracy is limited by the image resolution, the edge/contour pair having a distance less than two times of voxel size of the original source image can be regarded as successfully registered.

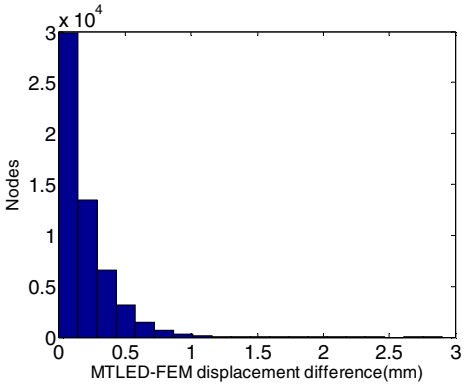

Fig. 3. Verification of the meshless model with fuzzy tissue classification used here for whole-body image registration. Differences between the nodal displacements predicted using the meshless model created in this study and previously validated [9] finite element model.

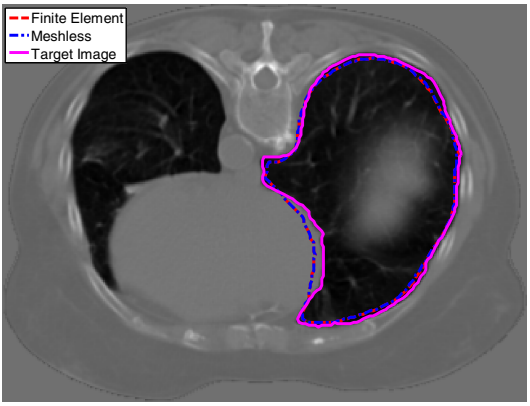

Fig. 4. Evaluation of registration accuracy. The dotted line and dashed line (they are nearly overlapping) represent lung contours extracted from images registered using deformations predicted by means of the meshless model used in this study and previously validated finite element model [9], respectively. The solid line is the lung contour extracted from the target image.

4 Discussion and Conclusions

In this study, we demonstrate feasibility of patient-specific computation of organ/tissue deformation for registration of whole-body CT images using meshless discretisation combined with fuzzy tissue classification. Unlike traditionally used finite element method, meshless discretisation (we used Meshless Total Lagrangian Explicit Dynamics MTLED algorithm with hexahedral background integration grid) facilitates automated and rapid generation of computational grid. Fuzzy tissue classification eliminates the need for tedious image segmentation to subdivide the image

into non-overlapping regions that correspond to different tissue types. Instead, the material properties are assigned at the integration points directly from the image. Fuzzy C-Means algorithm is adapted here to calculate the material properties using the fuzzy membership functions.

For the whole-body CT image dataset analysed in this study, the displacements predicted using the proposed meshless approach were very close to those previously obtained by Li et al. [9] using the validated finite element model. The organ contours in the registered (i.e. source image warped using deformations predicted by our patient-specific meshless model) image were close to the contours in the target image. The distance between the organ contours in the registered and target images was within the commonly used accuracy threshold of two times the voxel size.

Acknowledgments. The first author is a recipient of the SIRF scholarship and acknowledges the financial support of the University of Western Australia. The support of Australian Research Council (Discovery Grant DP120100402) is gratefully acknowledged. The whole-body CT image dataset analysed in this study was acquired from publically available Registration Library by National Alliance for Medical Image Computing (NA-MIC). NA-MIC is a national research centre supported by grant U54 EB005149 from the NIBIB NIH HHS Roadmap for Medical Research Program. The authors acknowledge contribution of Dr Guiyong Zhang (at present Dalian University of Technology, work done during appointment at The University of Western Australia) to development of the meshless code used in this study.

References

1. Warfield, S.K., Haker, S.J., Talos, I.F., Kemper, C.A., Weisenfeld, N., Mewes, A.U.J., Goldberg-Zimring, D., Zou, K.H., Westin, C.F., Wells, W.M., Tempany, C.M.C., Golby, A., Black, P.M., Jolesz, F.A., Kikinis, R.: Capturing intraoperative deformations: research experience at Brigham and Women's Hospital. Med. Image Anal. 9(2), 145–162 (2005)
2. Black, P.M., Moriarty, T., Alexander, E., Stieg, P., Woodard, E.J., Gleason, P.L., Martin, C.H., Kikinis, R., Schwartz, R.B., Jolesz, F.A.: Development and implementation of intraoperative magnetic resonance imaging and its neurosurgical applications. Neurosurgery 41(4), 831–842 (1997)
3. Mattes, D., Haynor, D.R., Vesselle, H., Lewellen, T.K., Eubank, W.: PET-CT image registration in the chest using free-form deformations. IEEE T. Med. Imaging 22(1), 120–128 (2003)
4. Goerres, G.W., Kamel, E., Heidelberg, T.N.H., Schwitter, M.R., Burger, C., von Schulthess, G.K.: PET-CT image co-registration in the thorax: influence of respiration. Eur. J. Nucl. Med. Mol. I 29(3), 351–360 (2002)
5. Hagemann, A., Rohr, K., Stiehl, H.S., Spetzger, U., Gilsbach, J.M.: Biomechanical modeling of the human head for physically based, nonrigid image registration. IEEE T. Med. Imaging 18(10), 875–884 (1999)
6. Chanthasopeephan, T., Desai, J.P., Lau, A.C.W.: Modeling soft-tissue deformation prior to cutting for surgical simulation: Finite element analysis and study of cutting parameters. IEEE T. Bio-Med. Eng. 54(3), 349–359 (2007)
7. Otoole, R.V., Jaramaz, B., Digioia, A.M., Visnic, C.D., Reid, R.H.: Biomechanics for Preoperative Planning and Surgical Simulations in Orthopedics. Computers in Biology and Medicine 25(2), 183–191 (1995)

8. Irving, G., Teran, J., Fedkiw, R.: Tetrahedral and hexahedral invertible finite elements. Graph Models 68(2), 66–89 (2006)
9. Li, M., Wittek, A., Joldes, G., Zhang, G., Dong, F., Kikinis, R., Miller, K.: Whole-Body Image Registration Using Patient-Specific Non-Linear Finite Element Model. In: Doyle, B.J., Miller, K., Wittek, A., Nielsen, P.M.F. (eds.) Computational Biomechanics for Medicine: Fundamental Science and Patient-Specific Application, pp. 21–30. Springer, New York (2013)
10. Wittek, A., Joldes, G., Couton, M., Warfield, S.K., Miller, K.: Patient-specific non-linear finite element modelling for predicting soft organ deformation in real-time; Application to non-rigid neuroimage registration. Prog. Biophys. Mol. Bio. 103(2-3), 292–303 (2010)
11. Miller, K., Horton, A., Joldes, G.R., Wittek, A.: Beyond finite elements: A comprehensive, patient-specific neurosurgical simulation utilizing a meshless method. J. Biomech. 45(15), 2698–2701 (2012)
12. Horton, A., Wittek, A., Joldes, G.R., Miller, K.: A meshless Total Lagrangian explicit dynamics algorithm for surgical simulation. Int. J. Numer. Meth. Bio. 26(8), 977–998 (2010)
13. Zhang, G.Y., Wittek, A., Joldes, G.R., Jin, X., Miller, K.: A three-dimensional nonlinear meshfree algorithm for simulating mechanical responses of soft tissue. Engineering Analysis with Boundary Elements 42, 60–66 (2014)
14. Zhang, J.Y., Joldes, G.R., Wittek, A., Miller, K.: Patient-specific computational biomechanics of the brain without segmentation and meshing. Int. J. Numer. Meth. Bio. 29(2), 293–308 (2013)
15. Balafar, M.A., Ramli, A.R., Saripan, M.I., Mashohor, S.: Review of brain MRI image segmentation methods. Artif. Intell. Rev. 33(3), 261–274 (2010)
16. Bezdek, J.C., Ehrlich, R., Full, W.: Fcm - the Fuzzy C-Means Clustering-Algorithm. Comput. Geosci. 10(2-3), 191–203 (1984)
17. Miller, K., Joldes, G., Lance, D., Wittek, A.: Total Lagrangian explicit dynamics finite element algorithm for computing soft tissue deformation. Commun. Numer. Meth. En. 23(2), 121–134 (2007)
18. Joldes, G.R., Wittek, A., Miller, K.: Suite of finite element algorithms for accurate computation of soft tissue deformation for surgical simulation. Med. Image Anal. 13(6), 912–919 (2009)
19. Fedorov, A., Beichel, R., Kalpathy-Cramer, J., Finet, J., Fillion-Robin, J.C., Pujol, S., Bauer, C., Jennings, D., Fennessy, F., Sonka, M., Buatti, J., Aylward, S., Miller, J.V., Pieper, S., Kikinis, R.: 3D Slicer as an image computing platform for the Quantitative Imaging Network. Magn. Reson. Imaging 30(9), 1323–1341 (2012)
20. Miller, K., Wittek, A., Joldes, G.: Biomechanical Modeling of the Brain for Computer-Assisted Neurosurgery. In: Miller, K. (ed.) Biomechanics of the Brain, pp. 111–136. Springer, New York (2011)
21. Fung, Y.C.: Mechanical Properties of Living Tissues. Springer, New York (1993) ISBN 978-1-4757-2257-4
22. Mostayed, A., Garlapati, R.R., Joldes, G.R., Wittek, A., Roy, A., Kikinis, R., Warfield, S.K., Miller, K.: Biomechanical Model as a Registration Tool for Image-Guided Neurosurgery: Evaluation Against BSpline Registration. Ann. Biomed. Eng. 41(11), 2409–2425 (2013)